Executive Summary of the Thesis

Techno-economic analysis and optimization of large-scale modular CSP tower plants

Laurea Magistrale in Energy Engineering - Ingegneria Energetica

Author: Rocco Manfredi Selvaggi

Advisor: Prof. Giampaolo Manzolini

Co-advisor: Giancarlo Gentile, Ettore Morosini

Academic year: 2021-2022

1. Introduction

Global warming and the consequences of the recent war have made evident the need for a large deployment of renewable technologies, which provide a cut in CO_2 emissions and secure from the high volatility of fossil fuel prices, ensuring a greater energy security. However, the growing share of variable renewable sources leads to grid issues, thus large-scale and cheap storage solutions are needed.

Concentrated Solar Power (CSP) includes a low-cost thermal energy storage system, allowing to decouple solar source from power generation and make the plant dispatchable. The state of the art is represented by 50-100 MW_{el} concrete tower plants with surrounding fields, cylindrical receivers, solar salts as heat transfer fluid (HTF), carried to the thermal energy storage (TES) by the piping system, and subcritical steam Rankine power blocks (PB).

Modular tower plants consist in multiple independent solar fields connected by a branched piping system to a centralized TES and PB. The rare studies in literature are quite discordant, and just few small-size plants exist worldwide. These are the Jemalong pilot plant (Australia) [1], built by Vast Solar and consisting of 5 rectangular polar modules to produce 1.1 MW_{el} and the Sierra SunTower plant (USA) [2], built by eSolar and made of 4 rectangular modules to produce 5 MW_{el}. Modularity allows for an optical efficiency increase and more compact plants, as well as exceeding the current size limit around 110 MW_{el}, allowing higher efficiency and economies of scale on the PB. Standardization guarantees lower installation complexity and construction time, while the smaller field's size allows for steel monopole towers derived from the wind industry, which reaches hub hights even beyond 160m. Some examples are the Sierra SunTower plant [2], with two 55m towers, and the Sundrop plant in Port Augusta (Australia) [3], with a 127m tower. In contrast, more towers and receivers are needed in modular plants, while the piping system is much larger.

In this study, a techno-economic analysis and optimization of large-scale modular plants is carried out, and a detailed Matlab model for the design of the related piping systems is built from scratch. Moreover, a precise methodology to investigate modular plants by means of the thermodynamic models of all components is set, and modules with different geometries and sizes are studied under different climatic conditions.

2. Methodology

To proceed with the analysis, thermodynamic models of the components are developed, along with a bottom-up methodology (Figure 1) for the design and optimization procedure. Starting from the climatic and geometric conditions of each module, the solar field is first generated, and the results in terms of power delivered to the receiver are used as inputs to the receiver models. Having applied this procedure to all modules, the minimum LCOH ones are then selected, and their number and geometry are used to run the piping model. Then, the power block model is also applied completing the analysis and allowing for the LCOE evaluation of the remaining options. Finally, the least-LCOE plant is selected.
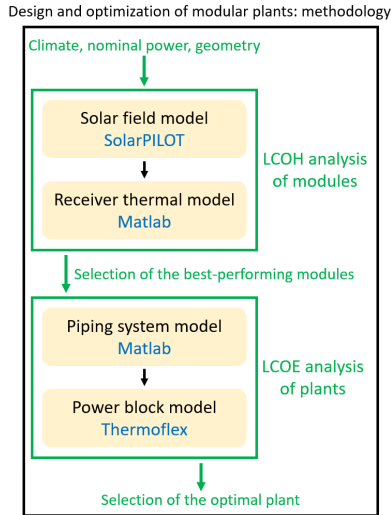

Figure 1: Schematic of the methodology

2.1. Solar field model

The solar field model is needed to obtain the design layout of the field and the annual operation, providing the heat flux on the receiver's external surface to be used on hourly basis in the receiver thermal model.

The main inputs of SolarPILOT models are climatic and geometric, while the outputs provide the field layout, the heat flux on the receiver, and the optical losses. The off-design provides optical efficiency maps as a function of the sun's azimuth and elevation angles.

The main parameters varied to generate modules, are design thermal power, field shape, receiver type (cylindrical or flat plate) and size, and tower height.

2.2. Receiver thermal model

The receiver model is based on the thermal model for cylindrical receivers described in [4]. This is a 2D model entirely developed in Matlab and allows the sizing and evaluation of thermal and pressure losses of both cylindrical and Billboard receivers starting from its dimensions and the heat flux maps from SolarPILOT. These are discretized and interpolated to obtain elementary fluxes matching the tubes' discretization. The off-design provides efficiency curves as a function of the thermal flux. For each module, first the tubes' diameter optimization is applied, employing standard diameters. Then the design and off-design models are run, obtaining the thermal powers transferred to the HTF and the receiver pressure drops, which are inputs of the piping model.

2.3. Piping model

A Matlab model is developed from scratch to assess thermal losses, pressure losses, and costs of the piping system in both design and annual conditions. This model receives as inputs the outputs of the receiver model (thermal power and pressure drops) and the geometry of modules from the solar field model, allowing to assess the impact of piping on the overall plant. The model can be used for any number of modules, size, field layout, and HTF, allowing to represent every configuration within a checkerboard layout. The working principle is based on the assimilation of modules to rectangles. It is assumed that all modules have the same geometry, operate under the same conditions, and that the riser and the downcomer are adiabatic. The land occupied by each module is counted as the rectangle that inscribes its shape, while for conventional plants, the land bounded by the outermost heliostats is considered. The space occupied by TES and PB in conventional systems is calculated as the circular region within the minimum field radius. In the modular case, if this region is located at the field's boundaries the area is equal to the conventional case, otherwise a surface equal to one module is accounted for. A new parameter is introduced, the land-specific productivity (LSP), to represent the plant's compactness in the electricity production, or even the effectiveness of the plant's land use.

$$LSP = \frac{AEP}{Land} \ [GWh/\mathrm{km}^2 y]$$

The order of the calculations follows the HTF path from the cold tank to the hot tank, by invoking two secondary functions for each straight pipe between two intersections. First the geometry is designed and the thermal losses are calculated, then the pressure losses are computed. The design code, whose frame is like the one developed in [5], and the scheme of a generic piping system are shown in Figure 2.
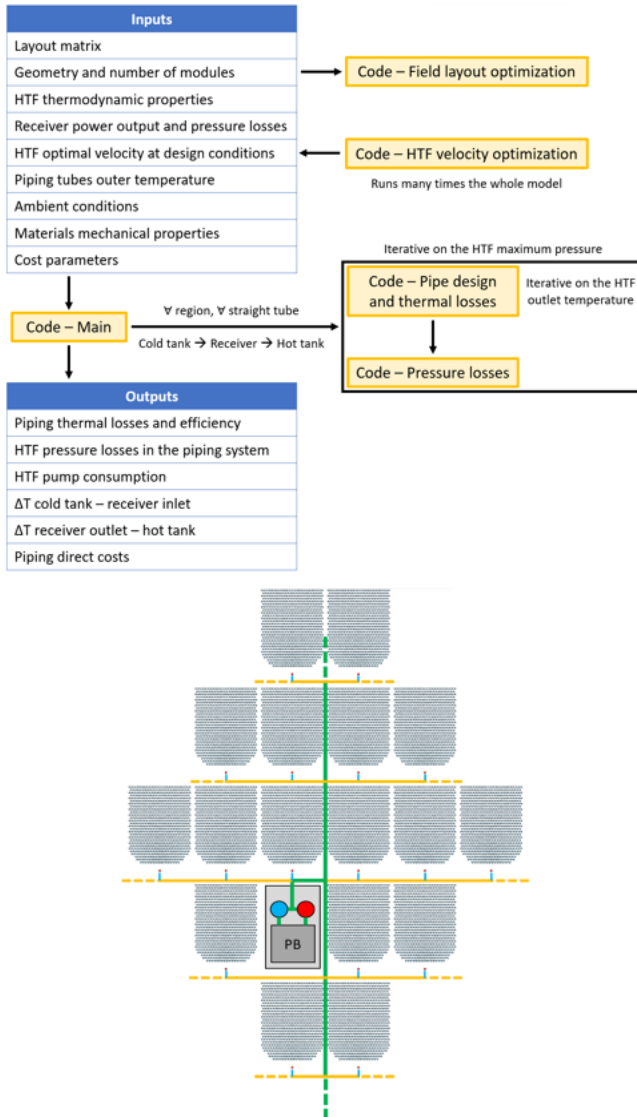

Figure 2: Flow diagram of the piping model and example of the system's modelling

The inner diameter of the duct D_{in} of each section is computed from the HTF velocity v_{HTF} knowing the mass flow rate m_{HTF}, while the thickness t is computed to resist to the maxi-

mum pressure with a security factor F = 1.5.

$$D_{in} = \sqrt{\frac{4 \cdot m_{HTF}}{\pi \cdot \rho_{HTF} \cdot v_{HTF}}}$$

$$t = \frac{(P_{max} - P_{amb}) \cdot D_{in}}{2 \cdot \frac{\sigma_{adm}}{F} + 0.4 \cdot (P_{max} - P_{amb})}$$

Where P_{max} is the maximum pressure at the exit of the HTF pump, computed iteratively, P_{amb} is the ambient pressure and σ_{adm} is the admissible normal stress. In addition, the expansion loops' number and length for accommodating the piping thermal expansion are also computed. The material adopted is stainless steel 316, and two insulating layers of mineral fiber with different maximum temperatures (600°C and 300°C) are included. The design is made imposing a piping outer temperature at design conditions $T_{ext,des}$, that must be low for reducing thermal losses and for safety reasons.

Starting from the inner tube diameter, a thermal resistance network (Figure 3) is computed to establish the diameters of the insulation layers $D_{out,mf1|2}$ to achieve the external temperature at the outer surface, with an iterative procedure on the HTF temperature at the tube's outlet T_{out}.
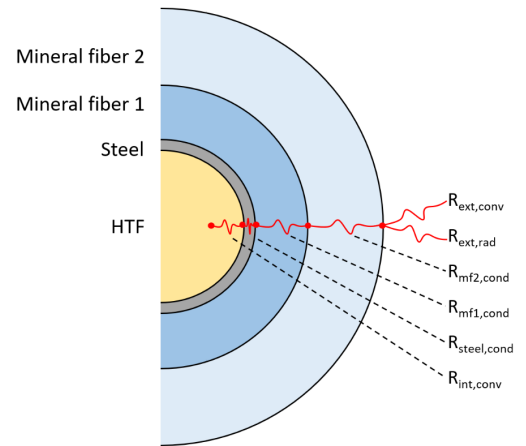

Figure 3: Tube's thermal resistance network

The thermal losses are calculated from the total resistance and the average fluid temperature T_{av} between inlet and outlet. The main equations of this procedure are reported below.

$$h_{in} = \frac{Nu_{HTF} \cdot k_{HTF}}{D_{int}}$$

$$h_{out} = h_{mix} + h_{rad}$$

$$R_{in|out} = \frac{1}{\pi \cdot D_{in,steel|out,mf2} \cdot h_{in|out}}$$

$$R_{steel|mf1,2} = \frac{\ln \frac{D_{out,steel|mf1,2}}{D_{in,steel|mf1,2}}}{2 \cdot \pi \cdot k_{steel|mf1,2}}$$

$$R_{tot} = R_{in} + R_{steel} + R_{mf1} + R_{mf2} + R_{out}$$

$$Q_{loss} = (T_{av} - T_{amb}) \cdot \frac{L_{pipe}}{R_{tot}}$$

$$T_{out,new} = T_{in} - \frac{Q_{loss}}{m_{flow} \cdot c_p}$$

For the internal convection, the Petukhov-Gnielinsky correlation is adopted to obtain the Nusselt number for solar salts. Finally, a constant $h_{mix} = 10$ W/m^{2}K is assumed for the combined natural and forced convection with the external environment, while the radiative losses are almost negligible due to the low temperature difference and the low-emissivity external aluminium foil cladding.

The maximum pressure difference provided by the HTF pump is the head required to overcome the piping and receiver pressure drops, assuming regulation valves at the base of each tower for ensuring isobaric mixes. The concentrated and distributed pressure losses are computed for each section once the diameters, the flow rates and the velocities are known. For concentrated pressure losses, elbows, combining and dividing T and X junctions are modelled. The loss coefficients for T junctions are obtained by interpolation of tabulated values, while X junctions are modelled as the combination of two T junctions. All the elbows are assumed to be flanged with a 90° curvature, and their loss coefficients are obtained from literature, from a correlation function of the Reynolds number Re:

$$K_{elbow} = 1.49 \cdot Re^{-0.145}$$

The implicit Colebrook equation is computed iteratively to determine the friction factor f for distributed pressure losses:

$$\frac{1}{\sqrt{f}} = -2 \cdot \log \left(\frac{2.51}{Re \cdot f} + \frac{\varepsilon}{D_{in} \cdot 3.72} \right)$$

Where ϵ is the roughness of stainless steel. Finally, the total pressure losses are the sum of concentrated and distributed losses:

$$P_{loss} = \left(K_{minor} + f \cdot \frac{L_{pipe}}{D_{int}} \right) \cdot \rho_{HTF} \cdot \frac{v_{HTF}^2}{2}$$

Where K_{minor} is the sum of all concentrated loss coefficients in the pipe under analysis.

The optimal HTF velocity at design conditions is computed minimising either the piping system's total losses or the specific cost of the power transferred. The off-design investigates the piping efficiency and the pump power as a function of the power transferred and the ambient temperature. A negligible dependency from the latter is observed since it induces a contextual decrease in the outermost insulation layer's thermal conductivity. Finally, the HTF pump's off-design efficiency is computed from a simplified approach proposed in literature:

$$\eta_{pump,off} = \eta_{pump,des} \left(2 \left(\frac{m_{off}}{m_{des}} \right) - \left(\frac{m_{off}}{m_{des}} \right)^2 \right)$$

2.4.   Power block model

The PB model is developed in [6] on Thermoflex. This is a 1-reheat subcritical steam Rankine cycle, then modified to derive a 2-reheats model. The need is to investigate the design and annual operation of this component to evaluate its performances and costs. For each cycle's layout, a desired net electric power is set as input to get the cycle efficiency as output. This efficiency allows to evaluate the thermal power needed to run the PB, which is necessary to properly size the TES and to evaluate the solar multiple, allowing to complete the plant's design. In off-design conditions, the cycle's performance curves are obtained at constant power input, as the ambient temperature varies. The partial load operation is not studied since the PB only works at full load, due to the TES strategy.

2.5.   Plants design

To design and optimize a modular CSP plant, the procedure is divided into independent and consecutive steps, making the process straightforward and avoiding iterative loops (Figure 4). First, many modules are defined in terms of geometry and power on the receiver.

The optimized modules are compared in terms of performances through the combined (optical·thermal) efficiency, while few suboptimal solutions are selected starting from the least-LCOH module. The LCOH [\$/MWh$_{th}$] is defined as:

$$LCOH = \frac{CAPEX_{sf} \cdot CRF}{AHP}$$

Then, the number of best-performing modules is set to obtain the desired electric power, and the
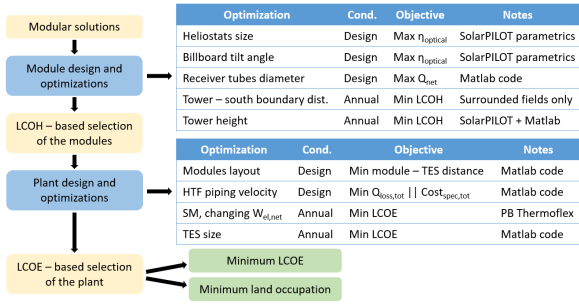
Modular solutions → **Module design and optimizations** → **LCOH – based selection of the modules** → **Plant design and optimizations** → **LCOE – based selection of the plant** → **Minimum LCOE** / **Minimum land occupation**

Optimization	Cond.	Objective	Notes
Heliostats size	Design	Max $\eta_{optical}$	SolarPILOT parametrics
Billboard tilt angle	Design	Max $\eta_{optical}$	SolarPILOT parametrics
Receiver tubes diameter	Design	Max Q_{net}	Matlab code
Tower – south boundary dist.	Annual	Min LCOH	Surrounded fields only
Tower height	Annual	Min LCOH	SolarPILOT + Matlab

Optimization	Cond.	Objective	Notes
Modules layout	Design	Min module – TES distance	Matlab code
HTF piping velocity	Design	Min $Q_{loss,tot}$ || $Cost_{spec,tot}$	Matlab code
SM, changing $W_{el,net}$	Annual	Min LCOE	PB Thermoflex
TES size	Annual	Min LCOE	Matlab code

Figure 4: Design of a modular plant

optimal plant is selected employing the LCOE [\$/MWh$_{el}$] as the parameter of merit:

$$LCOE = \frac{CAPEX_{plant} \cdot CRF + OPEX}{AEP}$$

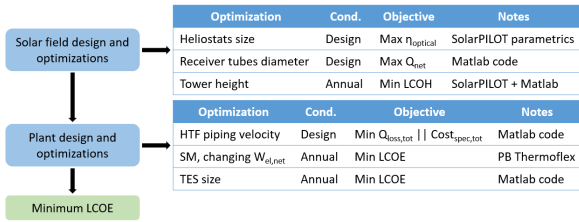Finally, the conventional plant's optimization is simpler since the solar field is unique (Figure 5).

Solar field design and optimizations → **Plant design and optimizations** → **Minimum LCOE**

Optimization	Cond.	Objective	Notes
Heliostats size	Design	Max $\eta_{optical}$	SolarPILOT parametrics
Receiver tubes diameter	Design	Max Q_{net}	Matlab code
Tower height	Annual	Min LCOH	SolarPILOT + Matlab

Optimization	Cond.	Objective	Notes
HTF piping velocity	Design	Min $Q_{loss,tot}$ || $Cost_{spec,tot}$	Matlab code
SM, changing $W_{el,net}$	Annual	Min LCOE	PB Thermoflex
TES size	Annual	Min LCOE	Matlab code

Figure 5: Design of a conventional plant

3. Case study

The locations for the main case study are Tucson (Arizona, USA), being representative for most CSP plants worldwide, and Calgary (Alberta, Canada), deliberately uncommon for CSP with very high latitude, to investigate the variation of the optical optimum and to determine if modularity ensures CSP feasibility even in locations now considered too expensive. Three scenarios are defined. In each, modular fields are investigated both according to the design power and to their geometry and layout (Figure 6). Each one is compared to a conventional plant at constant electric power, while a study up to 500 MW$_{el}$ is carried out in the most representative case.
The analysis of a hazy sky scenario is aimed at verifying the benefits of modularity under possible unfavourable conditions due to desert locations. In addition, square fields are chosen due to their symmetry and to limit land consumption, aiming to verifying whether this compensates the optical efficiency reduction. Table 1 reports the most important technical and

Low latitude (Tucson) *typical location for CSP*
- Latitude 32.1°
- DNI 2636 kWh/m²y
- Clear day atm. attenuation
- Hazy day atm. attenuation

High latitude (Calgary) *extreme location*
- Latitude 51.1°
- DNI 1819 kWh/m²y
- Clear day atm. attenuation

To investigate the variation of the optimal conditions with latitude and the modular CSP feasibility in locations now considered too expensive

Tucson clear Power [MW$_{th}$] 25, 50, 100, 150, 200, 250, 300, 350, 400

Tucson hazy Power [MW$_{th}$] 25, 50, 100, 200

Calgary (clear) Power [MW$_{th}$] 25, 50, 100, 150, 200, 300, 400

3 scenarios / Many powers

5 modules for each scenario and power

Surrounded field (cylindrical rec.) → Radial stagger layout → Free shape ① / Square shape ②
Polar field (Billboard rec.) → Radial stagger layout → Free shape ③ / Square shape ④
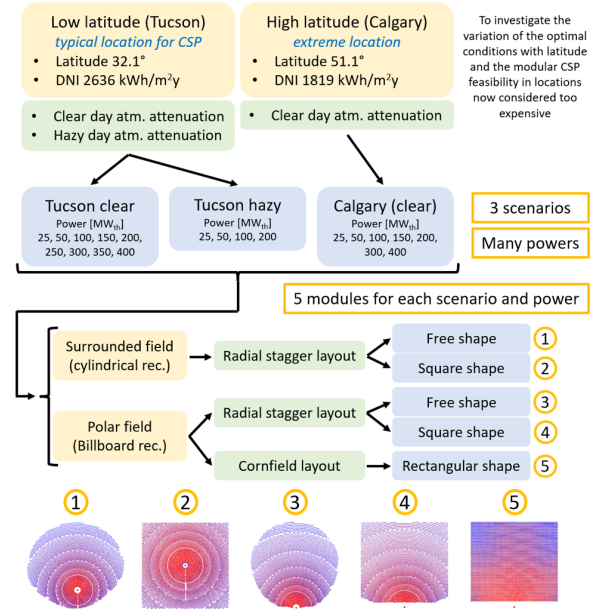→ Cornfield layout → Rectangular shape ⑤

Figure 6: Decision tree for the cases analysed

economic parameters, while in Table 2 the cost functions are shown. The economic analysis is subject to uncertainty, since for CSP it is quite difficult to find updated costs.

Max. H of steel towers [m]	150
Solar salts T range [°C]	$565 - 290$
Piping external T [°C] T. | C.	30 | 20
1-RH | 2-RH PB max. P [bar]	170 | 190
Heliostats [\$/m$^2_{hel}$]	100
TES + HTF pump [\$/kWh$_{th}$]	22

Table 1: Main technical and economic data

Tow. co. [M\$]	C=3·$e^{0.0113 \cdot H}$
Tow. st. [M\$]	C=1.5-0.009· H+0.0002· H^2
Rec. cyl. [M\$]	C=103· (A[m^2]/1571)$^{0.7}$
Rec. Bil. [M\$]	C=16.3· (A[m^2]/137.1)$^{0.7}$
Piping [\$]	C=C$_{mat}$+C$_{val}$+C$_{htf}$+C$_{sup}$
PB [M\$] [6]	Thermoflex cost· 1.49

Table 2: Cost functions

4.   Results

The tower location in surrounded modules is optimized as a function of the ratio y/Y between the distance tower - field's south side (y) and the total North-South extension of the module (Y). An example is shown in Figure 7.
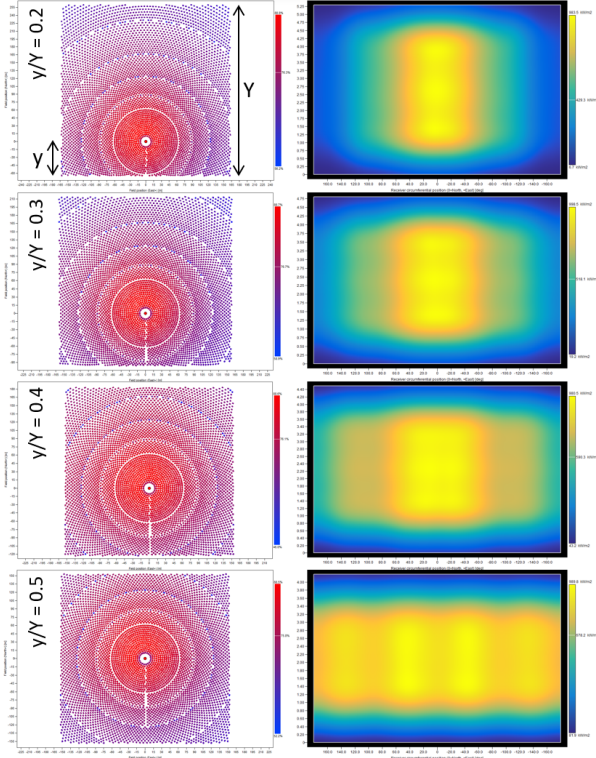

Figure 7: Field layout and flux map varying the tower location for square surrounded modules

Both in the case of free and square-shaped modules, a decreasing receiver size by moving the tower toward the centre is caused by an average flux increase, leading to a thermal efficiency increase and a cost reduction. Even if the combined efficiency peaks at y/Y=0.4 at low latitude and y/Y=0.3 at high latitude due to the cosine effect, the minimum LCOH always correspond to modules with the tower at y/Y=0.5. Thus, from a techno-economic perspective, it is always convenient to place the tower exactly in the centre of surrounded modules.

Considering the performances of all modules under study, a remarkable result is the great improvement of polar fields' optical efficiency by increasing latitude due to the cosine effect. Including the economic part, polar modules reveal lower LCOH than surrounded ones, while square modules result slightly more competitive than free-shape ones.

As for the piping system, the two modular configurations analysed are shown in Figure 8 and the main results are reported in Table 3.
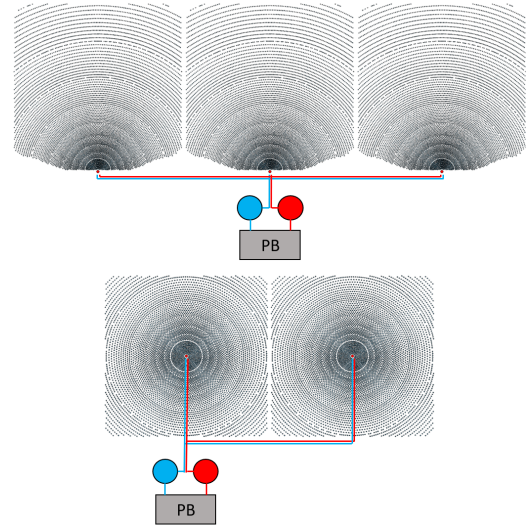

Figure 8: Modular layouts under study

The annual thermal efficiency is slightly lower in the modular plants, but still very high in absolute terms due to the low external piping temperature. Specific costs are 40% - 60% higher for modular plants. Finally, the annual auxiliary efficiency, which is entirely due to the HTF pump consumption, reveals the compensation between piping pressure losses (higher in modular plants) and receiver pressure losses (higher in the conventional case) since the values are very similar in all cases.

T. c.	3x300 P	2x400 S	900 C
$\eta_{th,ann}$ [%]	99.6	99.6	>99.9
$\eta_{aux,ann}$ [%]	98.0	97.7	97.6
C_{sp} [$/kW$_{el}$]	164	160	118
C.	3x300 P	2x400 S	900 C
$\eta_{th,ann}$ [%]	99.5	99.5	>99.9
$\eta_{aux,ann}$ [%]	98.0	97.2	97.5
C_{sp} [$/kW$_{el}$]	190	233	120
T. h.	-	2x200 S	400 C
$\eta_{th,ann}$ [%]	-	99.5	>99.9
$\eta_{aux,ann}$ [%]	-	98.0	98.1
C_{sp} [$/kW$_{el}$]	-	111	67

Table 3: Piping results

In conclusion, modular systems have higher piping losses and costs than conventional plants. However, in the case of plants around 100-110 MW$_{el}$, their magnitude is almost negligible compared to the overall plants.

The main plant-level results are given in Table 4. Conventional plants always have lower annual solar-to-electric efficiency than modular ones. Moreover, they do not have the lowest specific costs in any case because the lower receiver's cost is offset by the concrete tower, more expensive than steel monopole ones. In terms of compactness, 2 square surrounded modules bring great benefits, while 3 polar modules are less compact than the conventional case at low latitudes. Furthermore, a modular plant with 3 square polar fields provides LCOE reductions at all latitudes, while 2 square surrounded modules are convenient with hazy sky for smaller sizes.

T. c.	3x300 P	2x400 S	900 C
P$_{el}$	110	100	110
$\eta_{s-el,ann}$	18.0	17.6	17.4
LSP	68 (-20%)	130 (+53%)	85
LCOE	94 (-4.0%)	97 (-0.4%)	98
C.	3x300 P	2x400 S	900 C
P$_{el}$	100	90	100
$\eta_{s-el,ann}$	15.5	14.1	13.8
LSP	40 (+3%)	65 (+67%)	39
LCOE	144 (-5.6%)	154 (+1.1%)	152
T. h.	-	2x200 S	400 C
P$_{el}$	-	45	45
$\eta_{s-el,ann}$	-	16.0	15.4
LSP	-	114 (+27%)	90
LCOE	-	107 (-3.6%)	111

Table 4: Plant results: P$_{el}$ [MW$_{el}$], $\eta_{s-el,ann}$ [%], LSP [GWh/km^{2}y], LCOE [$/MWh$_{el}$]

Varying the net electric power at low latitudes towards 500 MW$_{el}$, the piping efficiency is almost constant as the number of modules increases. This is due to the increase in the local thermal efficiency of the main collectors, that compensates the low efficiency pipes added far from the TES to connect new modules.

The PB efficiency, instead, shows an increasing trend and a 1% improvement from 1 to 2 reheats. However, looking at the specific costs of these two components, the major impact of piping is shown (Figure 9).
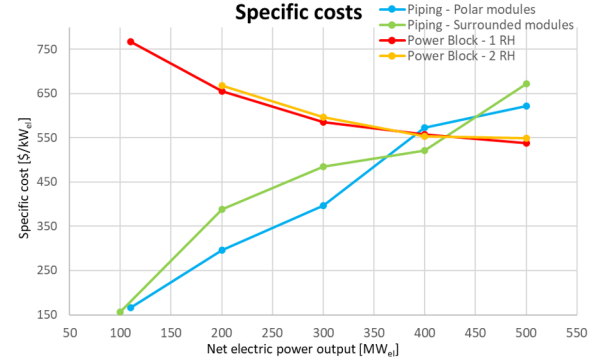

Figure 9: PB and piping specific costs

While the PB specific costs slightly decrease due to the economies of scale, the growth of the piping specific costs is evident. This is due to the addition of modules at an increasing distance from the TES, which leads to the necessity of larger amounts of material for the same power addition. Thus, the lowest LCOEs correspond to the smallest plants since the increase in the piping system's cost weighs more than the PB's improvements (Figure 10).
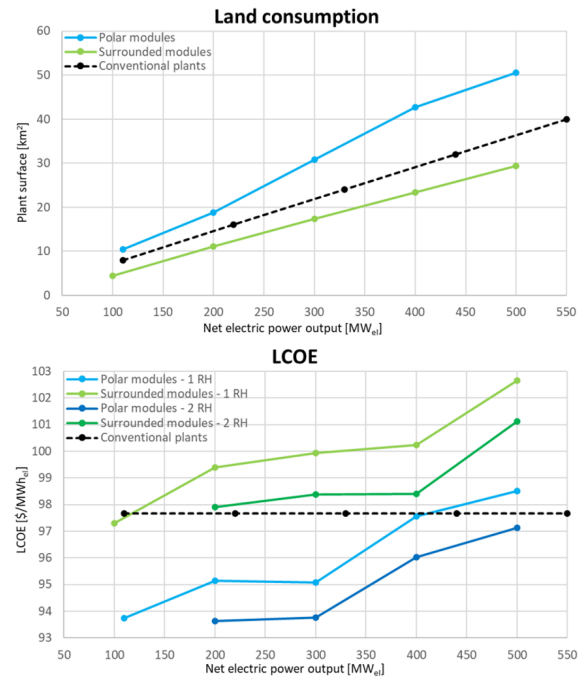

Figure 10: Land consumption and LCOE for modular plants and many conventional plants

This means that, even if modularity allows to overcome the conventional size limit of 110 MW_{el} caused by the subsequent optical decay, the piping system hinders the power size increase of CSP tower plants, limiting the achievement of 500 MW_{el} powers without increasing the LCOE. Other relevant results show that polar layouts are cheaper but larger than conventional plants, while surrounded ones are more expensive and compact. Finally, 2-reheat PBs allow for 300 MW_{el} plants without raising costs significantly.

5. Conclusions

A techno-economic analysis and optimization of large-scale modular CSP tower plants is carried out. A literature review highlights the existing modular plants, along with the advantages and drawbacks compared to the state-of-the-art. Then, thermodynamic models are described for solar field, receiver, piping, and PB.

A detailed Matlab model of the piping system is developed from scratch to assess its thermal losses, pressure losses and costs. This model is very flexible since it can be applied to any number of modules, size, and field layout. It is also essential to link the solar field and receiver models to the PB, ensuring the possibility to perform a detailed thermodynamic analysis of all components.

Then, a step-by-step bottom-up methodology and a cost model are defined to design and optimize both modular and conventional plants. The parameters of merit are LCOH, LCOE, and the new LSP, a specific indicator to compare the plants' compactness in producing electricity.

The major technical innovation consists in the combination of thermodynamic models of all components with a precise methodology and a cost model, making the whole modular plant's design and optimization a straightforward and accurate process, meanwhile simplifying the comparison with reference plants by means of few intensive indicators.

Modules of different sizes and geometries are then analysed in three scenarios at different latitude, DNI and atmospheric attenuation.

The results of the modules' design indicate that the optimal tower location in surrounded modules is always in the field centre, and that square modules are more competitive than free-shape ones in all cases and scenarios.

As for the piping, even if modular systems have higher losses and costs than conventional ones, the impact on the plant overall is almost negligible around 100 MW_{el}. The relevance of the piping system arises at larger powers, where specific costs significantly grow, overcoming the cost benefits provided by a larger PB. Therefore, while CSP modularity allows to go beyond the conventional plants' size due to its optical features, the piping system sets a new limit to the achievement of large powers typical of gas-fired or nuclear plants.

About the plants overall, large surrounded square modules are found to be much more compact than conventional CSP and equivalent PV plants, at the cost of a slightly higher LCOE. In contrast, large polar square modules are less compact but reduce the LCOE by 4%-6%. Finally, a 2-reheats Rankine PB allows for modular plants up to 300 MW_{el} without raising the LCOE.

References

[1] C. Wood, K. Drewes. *Vast Solar: improving performance and reducing cost and risk using high temperature modular arrays and sodium heat transfer fluid.* 2019.

[2] S. Schell. "Design and evaluation of eSolar's heliostat fields". In: *Solar Energy* 85 (4 Apr. 2011), pp. 614–619. ISSN: 0038092X. DOI: 10.1016/j.solener.2010.01.008.

[3] SunDrop. *Overview of Sundrop Farms.* Oct. 2017.

[4] G. Gentile et al. "Dynamic thermal analysis and creep-fatigue lifetime assessment of solar tower external receivers". In: *Solar Energy, under review.* (2022).

[5] K. Cooreman Magnus. "Techno-Economic Analysis of Multi-Tower Solar Thermal Power Plants". In: (2021).

[6] D. Belverato. "Off-Design analysis of Steam Rankine Cycles for CSP application". In: (2021).